0026-895X/05/6706-1977–1990$20.00
MOLECULAR PHARMACOLOGY
Vol. 67, No. 6
11676/3033782
Mol Pharmacol 67:1977–1990, 2005
Printed in U.S.A.

The Effects of Subunit Composition on the Inhibition of Nicotinic Receptors by the Amphipathic Blocker 2,2,6,6-Tetramethylpiperidin-4-yl Heptanoate

Roger L. Papke, Joshua D. Buhr, Michael M. Francis,[1] Kyung Il Choi,[2] Jeffrey S. Thinschmidt, and Nicole A. Horenstein

Department of Pharmacology and Therapeutics, College of Medicine, University of Florida, Gainesville, Florida (R.L.P., J.D.B., M.M.F., J.S.T.); and Department of Chemistry, University of Florida, Gainesville, Florida (K.I.C., N.A.H.)

Received February 1, 2005; accepted March 10, 2005

ABSTRACT

The therapeutic targeting of nicotinic receptors in the brain will benefit from the identification of drugs that may be selective for their ability to activate or inhibit a limited range of nicotine acetylcholine receptor subtypes. In the present study, we describe the effects of 2,2,6,6-tetramethylpiperidin-4-yl heptanoate (TMPH), a novel compound that is a potent inhibitor of neuronal nicotinic receptors. Evaluation of nicotinic acetylcholine receptor (nAChR) subunits expressed in *Xenopus laevis* oocytes indicated that TMPH can produce a potent and long-lasting inhibition of neuronal nAChR formed by the pairwise combination of the most abundant neuronal α (i.e., α3 and α4) and β subunits (β2 and β4), with relatively little effect, because of rapid reversibility of inhibition, on muscle-type ($\alpha1\beta1\gamma\delta$) or α7 receptors. However, the inhibition of neuronal β subunit-containing receptors was also decreased if any of the nonessential subunits α5, α6, or β3 were coexpressed. This decrease in inhibition is shown to be associated with a single amino acid present in the second transmembrane domain of these subunits. Our data indicate great potential utility for TMPH to help relate the diverse central nervous system effects to specific nAChR subtypes.

There are multiple types of nicotine acetylcholine receptors (nAChR) in the brain associated with synaptic function, signal processing or cell survival. The therapeutic targeting of nicotinic receptors in the brain will benefit from the identification of drugs that may be selective for their ability to activate or inhibit a limited range of these receptor subtypes. Mecamylamine is a ganglionic blocker developed many years ago as an antihypertensive and more recently suggested to be useful as a component in the pharmacotherapy for Tourette's syndrome (Sanberg et al., 1998) and smoking cessation (Rose et al., 1994). However, electrophysiological characterization of mecamylamine has shown it to be relatively nonselective (Papke et al., 2001), consistent with the observation that it effectively blocks all of the peripheral and central nervous system effects of nicotine (Martin et al., 1993). We previously identified a family of bis-tetramethylpiperidine compounds as inhibitors of neuronal type nicotinic receptors (Francis et al., 1998). The prototype compound in this series is BTMPS [bis-(2,2,6,6-tetramethyl-4-piperidinyl)-sebacate], which produces a readily reversible block of muscle-type nAChR and a nearly irreversible use-dependent, voltage-independent block of neuronal nAChR. The tetramethyl-piperidine groups of BTMPS are sufficient to produce block of nAChR, and the conjugation of two such groups with a long aliphatic chain accounts for both the selectivity and slow reversibility of BTMPS inhibition of neuronal nAChR (Francis et al., 1998). In the present study, we describe the effects of 2,2,6,6-tetramethylpiperidin-4-yl heptanoate (TMPH), a novel compound that has a single tetramethyl-piperidine group and an aliphatic chain similar to that of BTMPS. TMPH is also a potent inhibitor of neuronal nicotinic receptors.

Simple models for nAChR subtypes are provided by pairwise combinations of α and β subunits expressed in *Xenopus laevis* oocytes. However, there is a growing appreciation that ancillary subunits such as α5, α6, and β3 that work poorly in

This work was supported by National Institute on Drug Abuse grant DA017548; National Institutes of Health Grants NS32888, P01-AG10485, and MH11258; and the University of Florida College Incentive fund.
[1] Current address: Department of Biology, University of Utah, Salt Lake City, UT 84112.
[2] Current address: Korea Institute of Science and Technology, 39-1 Hawolgok-dong, Seongbuk-gu, Seoul, 136-791, Korea.
Article, publication date, and citation information can be found at http://molpharm.aspetjournals.org.
doi:10.1124/mol.105.011676.

ABBREVIATIONS: nAChR, nicotinic acetylcholine receptor; BTMPS, bis-(2,2,6,6-tetramethyl-4-piperidinyl)-sebacate; TMPH, 2,2,6,6-tetramethylpiperidin-4-yl heptanoate; TM, transmembrane; ACh, acetylcholine.

pairwise combinations with other single subunits, but nonetheless contribute to functionally important receptor subtypes in vivo. We show that for the commonly used nAChR subunit pairwise combinations inhibition by TMPH is only very slowly reversible. However, the incorporation of these additional subunits results in receptors that recover more rapidly and would thus show lower equilibrium inhibition in vivo. Therefore, based on the characterization of this agent's effects on specific nAChR subtypes, TMPH may identify the particular molecular substrates that underlie the multiple effects of nicotine in the brain.

Materials and Methods

Synthesis

Chemicals used for the synthesis were purchased from Aldrich Chemical Co. (Milwaukee, WI). Compounds were characterized by ^{1}H NMR and fast atom bombardment-mass spectrometry.

TMPH Synthesis. To a mixture of 2,2,6,6-tetramethyl-4-piperidinol (472 mg; 3.0 mmol) and methyl heptanoate (476 mg; 3.3 mmol) in 3.0 ml of dimethyl formamide was added 250 mg of powdered potassium carbonate. The resulting mixture was heated at ~145 to 155°C for 64 h under a gentle stream of N_2. After cooling, the reaction mixture was partitioned between water and hexanes. The organic layer was separated, washed with water (two times) and brine, and then dried over anhydrous $MgSO_4$ and evaporated to afford the crude product as an oil. The oil was dissolved in MeOH and was then treated with 2 equivalents of concentrated HCl. The solvent was removed in vacuo, and the residue was then treated with diethyl ether. The resulting solids were removed by filtration. The ethereal filtrate was concentrated in vacuo and triturated with hexane to afford 380 mg (41%) of TMPH hydrochloride. It was recrystallized from boiling ethyl acetate/hexane to afford short colorless needles, melting point 113 to 115°C. Fast atom bombardment-high resolution mass spectrometer: calculated($C_{16}H_{32}NO_2$): 270.2433 found: 270.2435.

Expression in *X. laevis* Oocytes

Mature (>9 cm) female *X. laevis* African frogs (Nasco, Ft. Atkinson, WI) were used as a source of oocytes. Before surgery, frogs were anesthetized by placing the animal in a 1.5 g/l solution of 3-aminobenzoic acid ethyl ester for 30 min. Oocytes were removed from an incision made in the abdomen.

To remove the follicular cell layer, harvested oocytes were treated with 1.25 mg/ml type 1 collagenase (Worthington Biochemicals, Freehold, NJ) for 2 h at room temperature in calcium-free Barth's solution (88 mM NaCl, 1 mM KCl, 0.33 mM $MgSO_4$, 2.4 mM $NaHCO_3$, 10 mM HEPES, pH 7.6, and 50 mg/l gentamicin sulfate). Thereafter, stage 5 oocytes were isolated and injected with 50 nl (5–20 ng) each of the appropriate subunit cRNAs. Recordings were made 2 to 15 days after injection.

Preparation of RNA. Rat neuronal nAChR clones and mouse muscle nAChR cDNA clones were used. The wild-type clones were obtained from Dr. Jim Boulter (UCLA, Los Angeles, CA). The rat α6/3 (Dowell et al., 2003) clone was obtained from Michael McIntosh (University of Utah, Salt Lake City, UT) and expressed in *X. laevis* oocytes in combinations with rat β2 and β3. The original α6/3 construct provided was sequenced and was found to have a mutation in the second transmembrane domain (TM2) sequence, which exchanged a valine for an alanine in the 7′ position (TM2 numbering scheme; Miller, 1989). The TM2 domain is understood to line the pore of the channel, with α helix structure. The 7′ position may actually be directed away from the actual pore lining, but this residue is highly conserved in all of the nAChRs. It is valine in all of them except α9 (isoleucine) and β1, where it is alanine. The TM2 mutation in the α6/3 chimera was corrected by using QuikChange (Stratagene, La Jolla, CA) according to their protocols. The corrected α6/3 chimera sequence was confirmed by restriction diagnostics and automated fluorescent sequencing (University of Florida core facility). The corrected clone was expressed as above in *X. laevis* oocytes with β2 and β3 and compared with the wild-type α3 coexpressed with β2 and β3. After linearization and purification of cloned cDNAs, RNA transcripts were prepared in vitro using the appropriate mMessage mMachine kit from Ambion (Austin, TX).

Electrophysiology. The majority of experiments were conducted using OpusXpress 6000A (Axon Instruments Inc., Union City, CA). OpusXpress is an integrated system that provides automated impalement and voltage clamp of up to eight oocytes in parallel. Cells were automatically perfused with bath solution, and agonist solutions were delivered from a 96-well plate. Both the voltage and current electrodes were filled with 3 M KCl. The agonist solutions were applied via disposable tips, which eliminated any possibility of cross-contamination. Drug applications alternated between ACh controls and experimental applications. Flow rates were set at 2 ml/min for experiments with α7 receptors and 4 ml/min for other subtypes. Cells were voltage-clamped at a holding potential of −60 mV. Data were collected at 50 Hz and filtered at 20 Hz. Agonist applications were 12 s in duration followed by 181-s washout periods for α7 receptors and 8 s with 241-s wash periods for other subtypes. For some experiments, particularly under conditions where residual inhibition precluded making repeated measurements from single cells (see below), manual oocyte recordings were made as described previously (Papke and Papke, 2002). In brief, Warner Instrument (Hamden, CT) OC-725C oocyte amplifiers were used, and data were acquired with a MiniDigi or Digidata 1200A with pClamp9 software (Axon Instruments Inc.). Sampling rates were between 10 and 20 Hz and the data were filtered at 6 Hz. Cells were voltage clamped at a holding potential of −50 mV. Data obtained with these methods were comparable with those obtained with OpusXpress.

Experimental Protocols and Data Analysis. Each oocyte received two initial control applications of ACh, an experimental drug application (or coapplication of ACh and TMPH), and then follow-up control application(s) of ACh. The control ACh concentrations for $\alpha1\beta1\gamma\delta$, $\alpha3\beta4$, $\alpha4\beta2$, $\alpha3\beta2$, $\alpha3\beta2\alpha5$, $\alpha3\beta2\beta3$, $\alpha6/3\beta2\beta3$ $\alpha6\beta4\beta3$, and $\alpha7$, receptors were 30, 100, 10, 30, 1, 100, 100, 100, and 300 μM, respectively. These concentrations were selected because they gave large responses with relatively little desensitization so that the same oocyte could be stimulated repeatedly with little decline in the amplitude of the ACh responses. This allowed us to separate out the inhibitory effects of the antagonist from possible cumulative desensitization.

Responses to experimental drug applications were calculated relative to the preceding ACh control responses to normalize the data, compensating for the varying levels of channel expression among the oocytes. Responses were characterized based on both their peak amplitudes and the net charge (Papke and Papke, 2002). In brief, for net charge measurement a 90-s segment of data beginning 2 s before drug application was analyzed from each response. Data were first adjusted to account for any baseline offset by subtracting the average value of 5-s period of baseline before drug application from all succeeding data points. When necessary, baseline reference was also corrected for drift using Clampfit 9.0 (Axon Instruments Inc.). After baseline correction, net charge was then calculated by taking the sum of all the adjusted points. The normalized net charge values were calculated by dividing the net charge value of the experimental response by the net charge value calculated for the preceding ACh control response. Means and S.E.M. were calculated from the normalized responses of at least four oocytes for each experimental concentration. To measure the residual inhibitory effects, this subsequent control response was compared with the preapplication control ACh response.

For concentration-response relations, data derived from net charge analyses were plotted using Kaleidagraph 3.0.2 (Abelbeck/

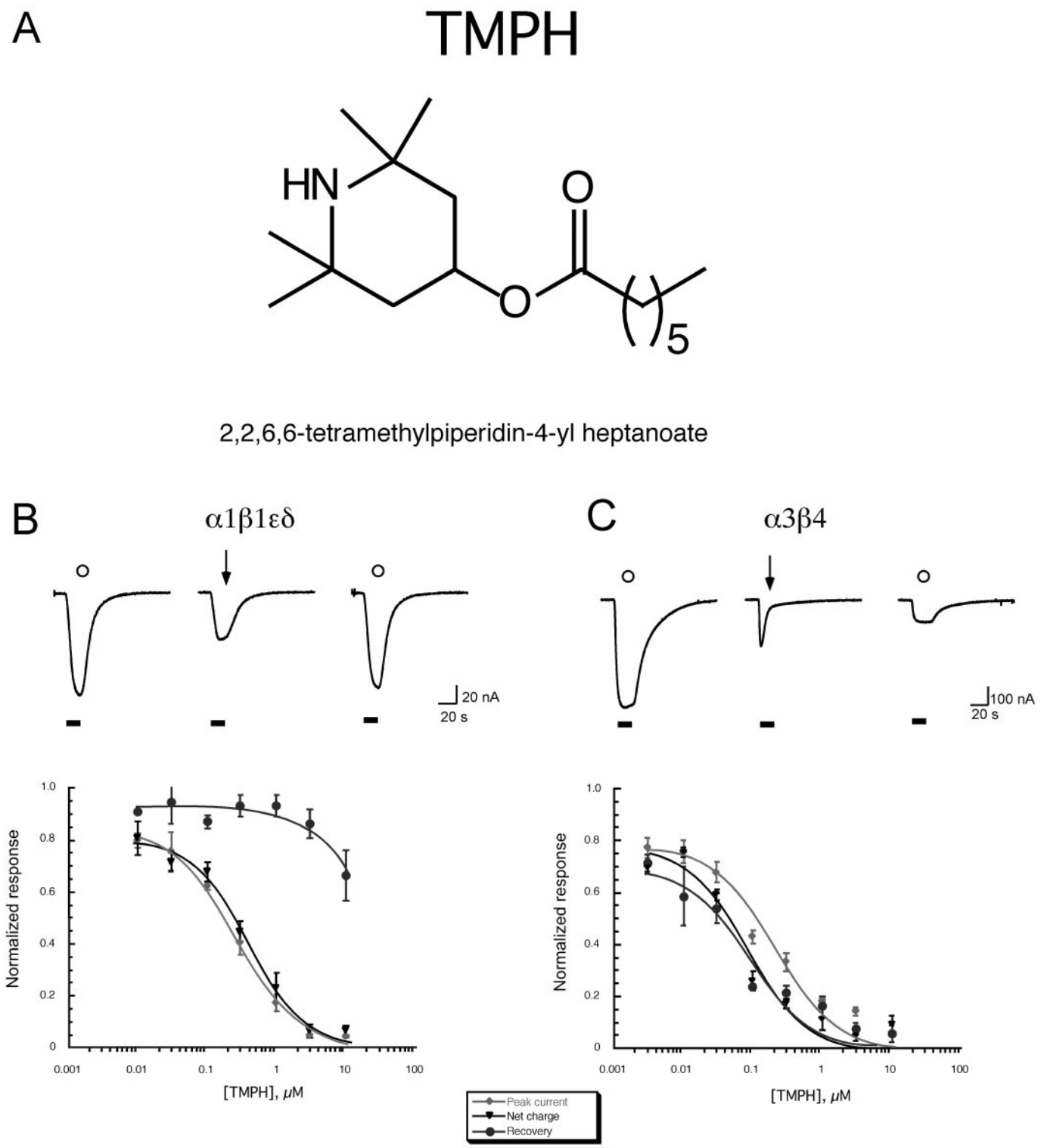

Fig. 1. TMPH produces selective long-term inhibition of neuronal ganglionic type $\alpha 3\beta 4$ receptors. A, chemical structure of TMPH. B, top, raw data traces obtained from an oocyte expressing mouse muscle-type $\alpha 1\beta 1\epsilon\delta$ subunits to the application of either 10 μM ACh alone (○) or the coapplication of 10 μM ACh and 300 nM TMPH (arrow). Bottom, averaged normalized data (±S.E.M.; $n \geq 4$) from oocytes expressing $\alpha 1\beta 1\epsilon\delta$ subunits to the coapplication 10 μM ACh and a range of TMPH concentrations. C, top, raw data traces obtained from an oocyte expressing rat ganglionic-type $\alpha 3\beta 4$ subunits to the application of either 100 μM ACh alone (○) or the coapplication of 100 μM ACh and 300 nM TMPH (arrow). Bottom, averaged normalized data (±S.E.M.; $n \geq 4$) from oocytes expressing $\alpha 3\beta 4$ subunits to the coapplication 100 μM ACh and a range of TMPH concentrations. Three values are plotted in each of the concentration-response curves: the peak current amplitude of the coapplication response, normalized to the peak amplitude of the previous ACh control (♦); the net charge of the coapplication response, normalized to the net charge of the previous ACh control (▼) (Papke and Papke, 2002) ; and the peak current amplitude of the ACh control response obtained after the TMPH/ACh coapplication, normalized to the peak amplitude of the previous ACh control (●).

Synergy, Reading, PA). Curves were generated from the Hill equation as follows:

$$\text{Response} = \frac{I_{max}[\text{agonist}]^n}{[\text{agonist}]^n + (EC_{50})^n}$$

where I_{max} denotes the maximal response for a particular agonist/subunit combination, and n represents the Hill coefficient. I_{max}, n, and the EC_{50} were all unconstrained for the fitting procedures. Negative Hill slopes were applied for the calculation of IC_{50} values.

Brain Slice Recording. Male Sprague-Dawley rats (p11-p20) were anesthetized with Halothane (Halocarbon Laboratories, River Edge, NJ) and swiftly decapitated. Transverse (300 mm) whole brain slices were prepared using a Vibratome and a high Mg^+/low Ca^{2+} ice-cold artificial cerebral spinal fluid containing 124 mM NaCl, 2.5 mM KCl, 1.2 mM NaH_2PO_4, 2.5 mM $MgSO_4$, 10 mM D-glucose, 1 mM $CaCl_2$, and 25.9 mM $NaHCO_3$ saturated with 95% O_2, 5% CO_2. Slices were incubated at 30°C for 30 min and then left at room temperature until they were transferred to a submersion chamber for recording. During experiments slices were perfused (2 ml/min) with normal artificial cerebral spinal fluid containing 126 mM NaCl, 3 mM KCl, 1.2 mM NaH_2PO_4, 1.5 mM $MgSO_4$, 11 mM D-glucose, 2.4 mM $CaCl_2$, 25.9 mM $NaHCO_3$, and 0.008 mM atropine sulfate saturated with 95% O_2, 5% CO_2 at 30°C. Medial septum/diagonal band cells were visualized with infrared differential interference contrast microscopy using a Nikon E600FN microscope. Whole cell patch-clamp recordings were made with glass pipettes (3–5 MΩ) containing an internal solution of 125 mM potassium gluconate, 1 mM KCl, 0.1 mM $CaCl_2$, 2 mM $MgCl_2$, 1 mM EGTA, 2 mM MgATP, 0.3 mM Na_3GTP, and 10 mM HEPES. Cells were held at −70 mV, and a −10 mV/10-ms test pulse was used to determine series and input resistances. Cells with series resistances >60 MΩ or those requiring holding currents >200 pA were not included in the final analyses. Local somatic application of 1 mM ACh and 1 mM ACh + 300 μM TMPH was performed using double barrel glass pipettes attached to a picospritzer (General Valve, Fairfield, NJ) with Teflon tubing (10–20 psi for 5–30 ms). For each cell, two baseline evoked responses to ACh were recorded followed by two evoked responses to ACh + TMPH (interstimulus interval of 30 s). ACh was then applied every 30 s for the remainder of the experiment. Signals were digitized using an Axon Digidata 1200A and sampled at 20kHz using Clampex version 9. Data analysis was done with Clampfit version 9.

Results

TMPH Inhibition of Acetylcholine Receptor Subtypes. TMPH (Fig. 1) was initially tested on mouse muscle-type ($\alpha1\beta1\epsilon\delta$) nAChR, three different pairwise combinations of rat neuronal α and β subunits ($\alpha3\beta4$, $\alpha4\beta2$, and $\alpha3\beta2$), and $\alpha7$ homomeric neuronal nAChR. In addition, combinations of three subunits and an $\alpha6/3$ chimera were tested. The results are summarized in Table 1. As shown in Fig. 1, both muscle-type and $\alpha3\beta4$ receptors (a minimal model for ganglionic-type receptors) were inhibited during the coapplication of ACh and TMPH. Although the inhibition of muscle-type receptors was readily reversible after a 5-min wash, the inhibition of $\alpha3\beta4$ receptors persisted after the wash. The data also indicate that the inhibition of $\alpha3\beta4$ receptors became progressively greater during the coapplication response so that the inhibition of net charge was greater than the inhibition of peak current. This was not the case for the inhibition of muscle-type receptors. The other neuronal α-β subunit pairs tested, $\alpha4\beta2$ and $\alpha3\beta2$, were blocked in a manner similar to $\alpha3\beta4$ receptors (Fig. 2), with a larger inhibition of net charge than peak current and virtually no recovery after a 5-min wash. In contrast, $\alpha7$ receptors, like muscle-type receptors, showed little difference between the inhibition of peak currents and net charge and showed significant recovery after a 5-min wash (Fig. 2). These differences are reflected in the IC_{50} values presented in Table 1. Note that receptors that rapidly equilibrate inhibition and recover readily (e.g., muscle-type receptors and $\alpha7$) have ratios of the IC_{50} for net charge to the IC_{50} for peak currents of close to 1 (Table 2). In contrast, for receptor types that show progressively more inhibition during the coapplication and have slow recovery, the ratio of the IC_{50} for net charge to the IC_{50} for peak currents is much less than 1. Therefore, for receptors that show progressively more inhibition during the coapplication IC_{50} values estimated from the inhibition of net charge are similar to those that can be derived from persistent inhibition measured after a 5-min wash (i.e., from the recovery data; Table 2).

Neuronal nAChR Recovery Rates. Our initial experiments evaluated recovery after only a single 5-min wash. To evaluate the actual rates at which $\alpha7$ and the various nAChR pairwise subunit combinations recovered from TMPH-induced inhibition, we made repeated applications of ACh alone after a single coapplication of ACh and TMPH. As shown in Fig. 3, the rat $\alpha4\beta2$, $\alpha3\beta2$, $\alpha3\beta4$ receptors showed virtually no detectable recovery over a period of 30 min, whereas $\alpha7$ receptors were fully recovered after approximately 15 min of wash.

TABLE 1

In vitro data

IC_{50} values were calculated based on either the decrease in peak current amplitudes or the decrease in the net charge of the ACh response when coapplied with TMPH. For many of the subunit combinations tested, there was no detectable recovery after a 5-min wash, so IC_{50} values were also calculated based on the inhibition still present at the 5-min time point (recovery). Note that these IC_{50} values are based on standard single application protocol and are likely to underestimate the IC_{50} for steady-state conditions.

Subunit	IC_{50} (Peak)	IC_{50} (Area)	IC_{50} (Recovery)
Mouse muscle	276 ± 20 nM	390 ± 50 nM	27 ± 5.5 μM
Rat $\alpha7$	1.0 ± 0.1 μM	1.2 ± 0.2 μM	16 ± 4 μM
Rat $\alpha4\beta2$	1.4 ± 0.3 μM	110 ± 40 nM	250 ± 80 nM
Rat $\alpha3\beta4$	200 ± 50 nM	75 ± 23 nM	85 ± 32 nM
Rat $\alpha3\beta2$	3.7 ± 1.2 μM	440 ± 90 nM	230 ± 30 nM
Human $\alpha3\beta2$	3.7 ± 1.2 μM	460 ± 170 nM	400 ± 120 nM
Human $\alpha3\beta2\alpha5$	1.1 ± 0.5 μM	430 ± 180 nM	750 ± 200 nM
Rat $\alpha3\beta2\beta3$	120 ± 80 μM	2.7 ± 0.6 μM	4.3 ± 1.5 μM
Rat $\alpha6/3\beta2\beta3$	60 ± 20 μM	1.0 ± 0.3 μM	2.3 ± 0.5 μM
Rat $\alpha3\beta4\beta3$	1.9 ± 0.2 μM	1.4 ± 0.2 μM	30 ± 50 μM, 1.0 ± 0.6 μM[a]
Rat $\alpha6\beta4\beta3$	11.0 ± 4.4 μM	18.3 ± 4.9 μM	1700 ± 420 μM

[a] Data for the recovery of cells expressing $\alpha3\beta4\beta3$ were fit to a two-site model (see Fig. 9).

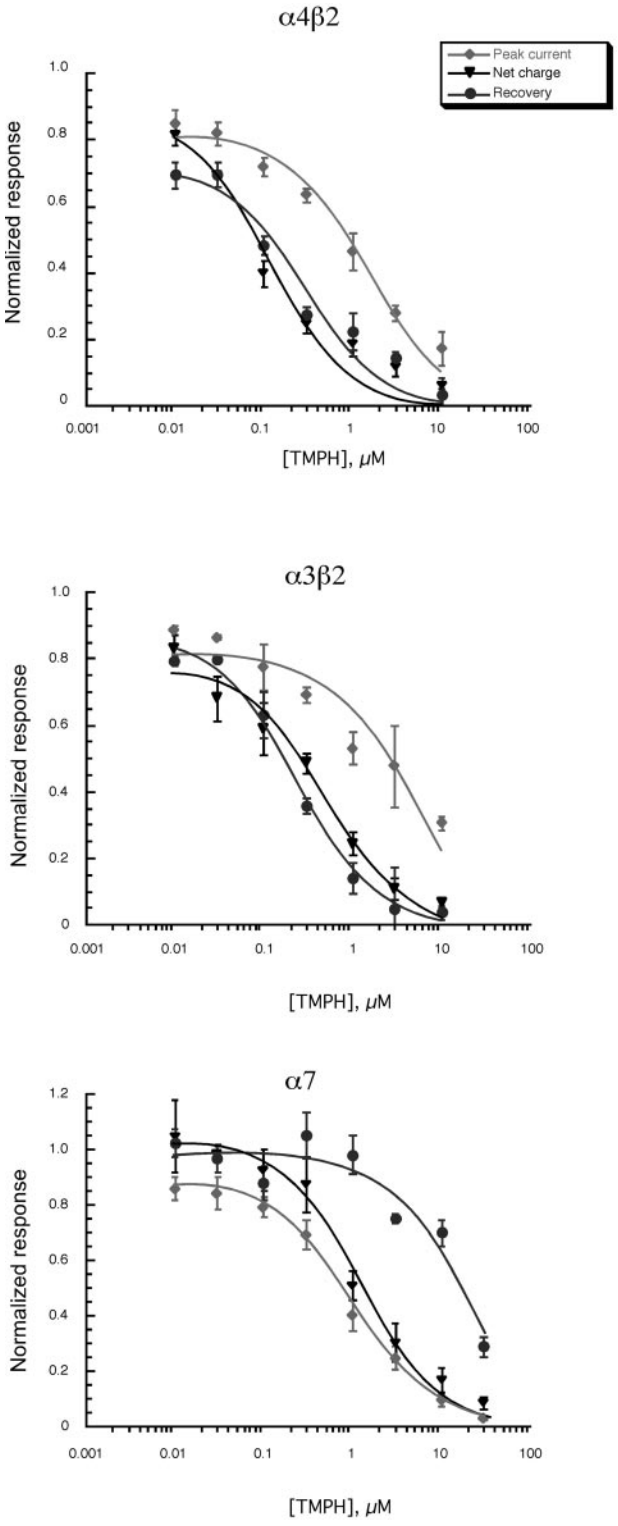

Fig. 2. TMPH inhibition of responses obtained from oocytes expressing rat neuronal nAChR subunits. Shown are the averaged normalized data (±S.E.M.; $n \geq 4$) from oocytes expressing $\alpha4\beta2$, $\alpha3\beta2$, and $\alpha7$ subunits (from top to bottom, respectively) to the coapplication ACh and a range of TMPH concentrations. Three values are plotted in each of the concentration-response curves: the peak current amplitude of the coapplication response, normalized to the peak amplitude of the previous ACh control (♦); the net charge of the coapplication response, normalized to the net charge of the previous ACh control (▼); and the peak current amplitude of the ACh control response obtained after the TMPH/ACh coapplication, normalized to the peak amplitude of the previous ACh control (●). The control ACh concentrations used were 10, 30, and 300 μM for $\alpha4\beta2$, $\alpha3\beta2$, and $\alpha7$, respectively.

Use Dependence of Inhibition by TMPH. We evaluated the degree to which inhibition by TMPH was use-dependent by applying 1 μM TMPH alone and comparing the response to a subsequent control ACh application to that obtained after 1 μM TMPH was coapplied with ACh. As shown in Fig. 4, the ability of TMPH to inhibit neuronal nAChR when applied in the absence of agonist varied significantly among the pairwise subunit combinations tested, but in all cases was less than when TMPH was coapplied with agonist. It is interesting that although TMPH alone applied to $\alpha4\beta2$ receptors was almost as effective as when coapplied with ACh, TMPH alone applied to $\alpha3\beta2$ receptors had no detectable effect after the washout period.

TABLE 2

In vitro data

The value IC_{50} recovery reflects the residual inhibition of the ACh control response measured after a 5-min wash. If IC_{50} recovery > IC_{50} area, then there was significant recovery (i.e. readily reversible inhibition). Likewise, if IC_{50} area < IC_{50} peak, then there was significant buildup of inhibition throughout the agonist/antagonist coapplication.

	IC_{50} (Net Charge/IC_{50} Peak)	IC_{50} (Recovery/IC_{50} Net Charge)
Mouse $\alpha1\beta1\delta\epsilon$	1.4	69
Rat $\alpha7$	1.2	13.3
Rat $\alpha4\beta2$	0.08	2.3
Rat $\alpha3\beta4$	0.36	1.1
Rat $\alpha3\beta2$	0.12	0.52
Human $\alpha3\beta2$	0.12	0.87
Human $\alpha3\beta2\alpha5$	0.15	1.7
Rat $\alpha3\beta2\beta3$	0.025	1.6
Rat $\alpha6/3\beta2\beta3$	0.017	2.0
Rat $\alpha3\beta4\beta3$	0.74	0.7, 21[a]
Rat $\alpha6\beta4\beta3$	1.7	93

[a] Data for the recovery of cells expressing $\alpha3\beta4\beta3$ was fit to a two-site model (see Fig. 9).

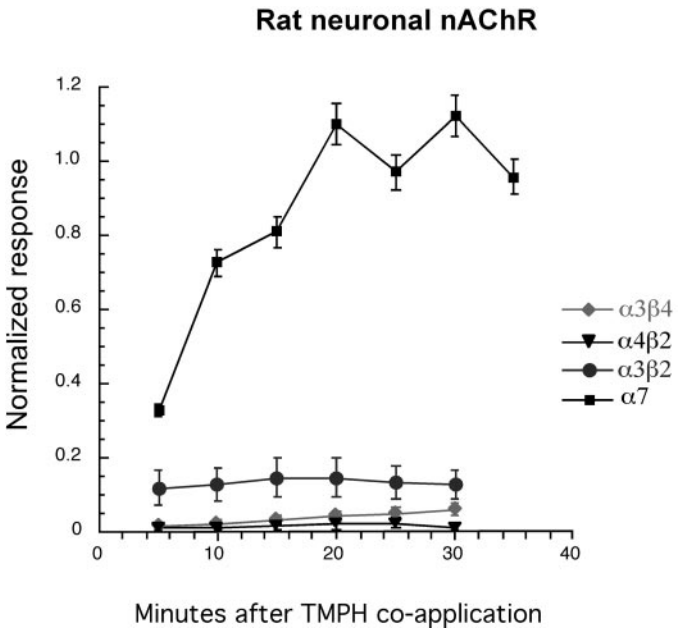

Fig. 3. TMPH produces long-term inhibition of neuronal beta subunit-containing nAChR but not $\alpha7$ homomeric receptors. ACh and TMPH were coapplied at time 0 to oocytes expressing rat $\alpha3\beta4$, $\alpha4\beta2$, $\alpha3\beta2$, or $\alpha7$ subunits. Thereafter, control ACh applications were made at 5-min intervals to measure recovery. The control ACh concentrations used were 100, 10, 30, and 300 μM for $\alpha3\beta4$, $\alpha4\beta2$, $\alpha3\beta2$, and $\alpha7$, respectively. The initial inhibition was produced by the coapplication of ACh at the control concentration and 30 μM TMPH, except in the case of the $\alpha3\beta2$ receptors, which were inhibited by the coapplication of ACh and 3 μM TMPH.

Progressive Inhibition of $\alpha4\beta2$ Receptors by Repeated Coapplications of ACh and TMPH below Its IC_{50} Value. The IC_{50} values presented in Table 1 were based on the inhibition produced by single coapplications (20 s in duration) of ACh and TMPH. Because for the neuronal β subunit-containing receptors the onset of inhibition is apparently much faster than the reversibility of inhibition, measurements based on single applications of TMPH are likely to underestimate what equilibrium IC_{50} values would be. To test the hypothesis that repeated applications of TMPH would produce an accumulated inhibition that would be greater than the inhibition produced by a single application, we made repeated coapplications of ACh and 100 nM TMPH to oocytes expressing $\alpha4\beta2$ receptors. Coapplications of TMPH and ACh were alternated with applications of ACh alone. As shown in Fig. 5, repeated coapplications of ACh with 100 nM TMPH (IC_{50} in single-dose experiments) produced 90% inhibition after three applications at 10-min intervals. Further applications did not produce additional inhibition. Making a corresponding shift in the $\alpha4\beta2$ net charge inhibition curve in Fig. 3 (i.e., so that 100 nM is the IC_{90} rather than the IC_{50}) suggests that the equilibrium IC_{50} would be approximately 10 nM.

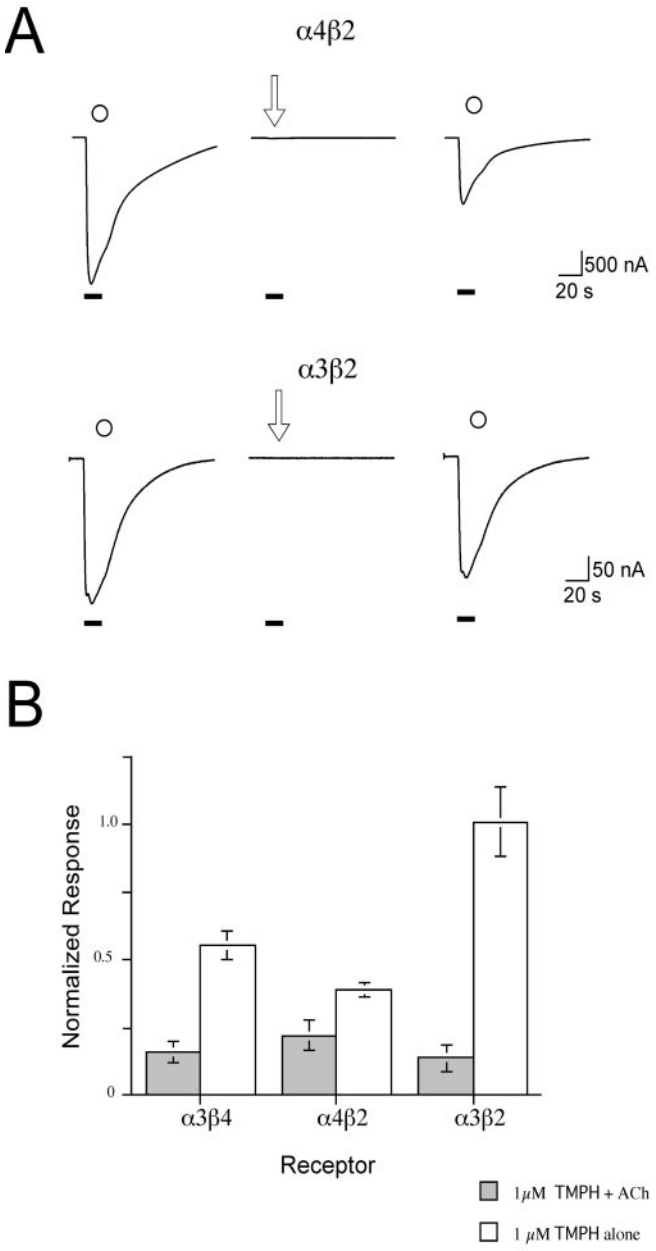

Fig. 4. Varying amounts of use-independent inhibition of neuronal β subunit-containing receptors by TMPH. A, representative data showing the effects of the application of 1 μM TMPH alone to $\alpha4\beta2$- and $\alpha3\beta2$-expressing oocytes (open arrows), compared with the application of ACh alone (○) either before or after the application of TMPH. The control ACh concentrations used were 10 and 30 μM for $\alpha4\beta2$ and $\alpha3\beta2$, respectively. B, comparison of the use-dependent (1 μM TMPH + ACh) and use-independent (1 μM TMPH alone) inhibition of $\alpha3\beta4$, $\alpha4\beta2$, and $\alpha3\beta2$ receptors by TMPH. The data are calculated from the peak amplitudes of control ACh responses obtained after the application of TMPH ± ACh, expressed relative to the peak current amplitude of ACh control responses before the application of TMPH.

Effect of $\alpha5$ Coexpression with $\alpha3\beta2$ Subunits on the Sensitivity to TMPH. As noted above, efforts to connect data obtained from oocyte studies with in vivo data can be complicated by the fact that nAChR in vivo may have more complex subunit composition than the simple pairwise α/β subunit combinations most readily tested in oocytes. One such subunit that contributes to the complexity of acetylcholine receptors in vivo is $\alpha5$, which is not required to coassemble with other subunits for them to function but is likely to be present in some receptor subtypes in vivo (Wang et al., 1996; Gerzanich et al., 1998). We tested the hypothesis that the presence of the $\alpha5$ subunit could modulate the sensitivity of a neuronal nAChR subunit to TMPH. For these experiments, we used human $\alpha3$ and $\beta2$ subunits, which readily form receptors with or without the coexpression of the human $\alpha5$ subunit. We chose to use these subunits because the successful inclusion of the $\alpha5$ subunit produces an easily detectable change in receptor pharmacology, increasing the potency of ACh (Gerzanich et al., 1998). All batches of oocytes used for these experiments were confirmed to have this predicted effect of $\alpha5$ expression.

As shown in Fig. 6, ACh responses of oocytes expressing human $\alpha3\beta2$ and human $\alpha3\beta2\alpha5$ showed similar sensitivity to TMPH during the initial coapplication. (The IC_{50} values based on net charge analysis were 460 ± 170 and 430 ± 180 nM, respectively.) However, as shown in Fig. 7, oocytes expressing $\alpha5$ along with $\alpha3$ and $\beta2$ showed much faster recovery than those expressing $\alpha3$ and $\beta2$ alone. The responses of oocytes expressing $\alpha3\beta2\alpha5$ had a half-time of recovery of approximately 15 min, whereas those expressing human $\alpha3\beta2$ receptors showed no significant recovery over a period of 40 min, similar to the oocytes expressing rat $\alpha3\beta2$ receptors (Fig. 3).

Inhibition of Receptors Containing $\beta3$ and $\alpha6$ Subunits. It has been suggested that in vivo $\beta3$ subunits may coassemble with $\alpha6$ and possibly $\alpha4$ and $\beta2$ to make receptors that regulate dopamine release (Champtiaux et al., 2003). However, the $\alpha6$ subunit expresses poorly in oocytes when used in pairwise combinations with beta subunits (Kuryatov et al., 2000). One approach to get around this problem has been to use a chimera of $\alpha6$ and $\alpha3$ that has improved expression properties. Because of the presence of the $\alpha6$ extracellular domain, receptors formed with this chimera are sensitive to $\alpha6$-selective competitive antagonists (Dowell et al., 2003). We compared the effects of TMPH on oocytes expressing $\alpha3\beta2\beta3$ and a chimera of $\alpha6$ and $\alpha3$ subunits, $\alpha6/3$ (Dowell et al., 2003) along with $\beta2$ and $\beta3$. This approach allowed

us to systematically evaluate first the effects of the $\beta 3$ subunits (by comparing oocytes injected with $\alpha 3\beta 2\beta 3$ to those expressing $\alpha 3\beta 2$ alone) and second the effects of the $\alpha 6$ extracellular domain (by comparing $\alpha 6/3\beta 2\beta 3$ with $\alpha 3\beta 2\beta 3$).

The addition of the $\beta 3$ subunit to the $\alpha 3$ and $\beta 2$ subunits had the effect of decreasing sensitivity to an initial application of TMPH (Fig. 8A) such that the IC_{50} for inhibiting $\alpha 3\beta 2\beta 3$ receptors was at least an order of magnitude higher than for the inhibition of $\alpha 3\beta 2$ without $\beta 3$ (Figs. 2 and 8; Table 1). The receptors containing the $\alpha 6/3$ chimera in combination with $\beta 2$ and $\beta 3$ were not significantly different in their sensitivity to TMPH from those made up of the $\alpha 3\beta 2\beta 3$ wild-type subunits (Fig. 8B; Table 1). The recovery of $\beta 3$-containing receptors from TMPH was relatively complex. There was approximately 50% recovery in the first 10 min, but no further recovery after that. This was similar for both $\alpha 3\beta 2\beta 3$ and $\alpha 6/3\beta 2\beta 3$ (Fig. 8C). One possible explanation for this would be if the coexpression of these subunits resulted in mixed populations of receptors, some containing $\beta 3$ subunits and showing rapid recovery, and others formed without $\beta 3$ and showing the nearly irreversible block seen when $\alpha 3$ and $\beta 2$ are expressed as a pair. This is certainly a likely scenario for the combination containing wild-type $\alpha 3$ and may also be the case for the combination containing the chimera, because in our experience there is an increase of approximately 2-fold in currents when $\beta 3$ is coexpressed with $\beta 2$ and the $\alpha 6/3$ chimera compared with $\alpha 6/3$ and $\beta 2$ alone (data not shown).

The data in Fig. 8 suggest that the $\beta 3$ subunit imparts some resistance to inhibition by TMPH and also that the extracellular domain of $\alpha 6$ has relatively little effect. We therefore tested oocytes expressing the complete wild-type $\alpha 6$ subunit. The $\alpha 6$ subunit was coexpressed with $\beta 4$ and $\beta 3$ because this is the only $\alpha 6$ combination we have found to work with any consistency. For these experiments, as a con-

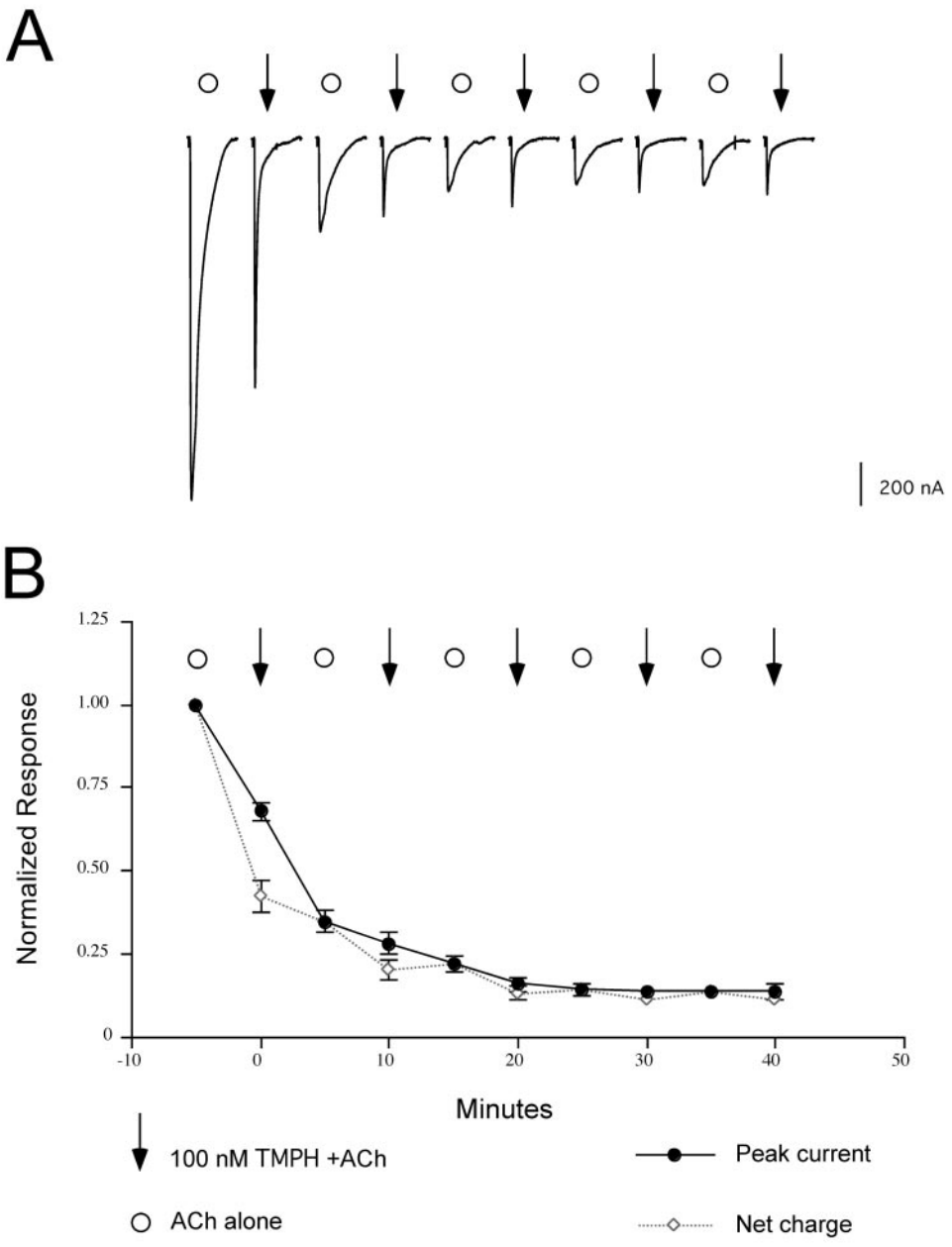

Fig. 5. Cumulative inhibition by repeated application of TMPH. A, responses of an oocyte expressing $\alpha 4\beta 2$ receptors to alternating applications of 30 μM ACh alone (○) or 30 μM ACh plus 100 nM TMPH (arrows). The total inhibition increased during the first 3 TMPH/ACh coapplications. Note that the TMPH/ACh coapplications differ in kinetics from the ACh controls, showing a greater inhibition of net charge than of peak current. B, normalized average responses of oocytes expressing $\alpha 4\beta 2$ receptors ($\pm$S.E.M.; $n \geq 4$) to alternating applications of ACh alone or ACh plus TMPH, as in A. Both peak currents and net charge values are plotted, normalized to the ACh control response recorded before the first ACh/TMPH coapplication ($t = -5$ min). Note that the traces in A are shown on the same time scale as the x-axis in B.

trol we compared the oocytes injected with $\alpha6\beta4\beta3$ to oocytes injected with $\alpha3\beta4\beta3$. As shown in Fig. 9, the oocytes expressing $\alpha6\beta4\beta3$ showed relatively weak inhibition by TMPH during the coapplication of TMPH and ACh, with an IC_{50} value for the inhibition of net charge nearly an order of magnitude higher than for any other receptor subunit combination tested (Table 1). This reduced sensitivity to TMPH was most probably caused by both the $\alpha6$ and the $\beta3$ subunits because $\alpha3\beta4\beta3$-injected oocytes were much less sensitive than those expressing $\alpha3\beta4$ alone.

The responses of oocytes expressing $\alpha6\beta4\beta3$ showed essentially full recovery after only a single wash period (Fig. 9B). However, as with the oocytes expressing $\alpha3$, $\beta2$, and $\beta3$, it is likely that the cells injected with $\alpha3$, $\beta4$, and $\beta3$ had a mixed population of receptors because the recovery data were best fit with a two-site model (Fig. 9A).

Sequence in the Pore-Forming TM2 Domain Regulates TMPH Inhibition. Although receptors containing pairwise combinations with either $\beta2$ or $\beta4$ showed nearly irreversible inhibition by TMPH, inclusion of any of the com-

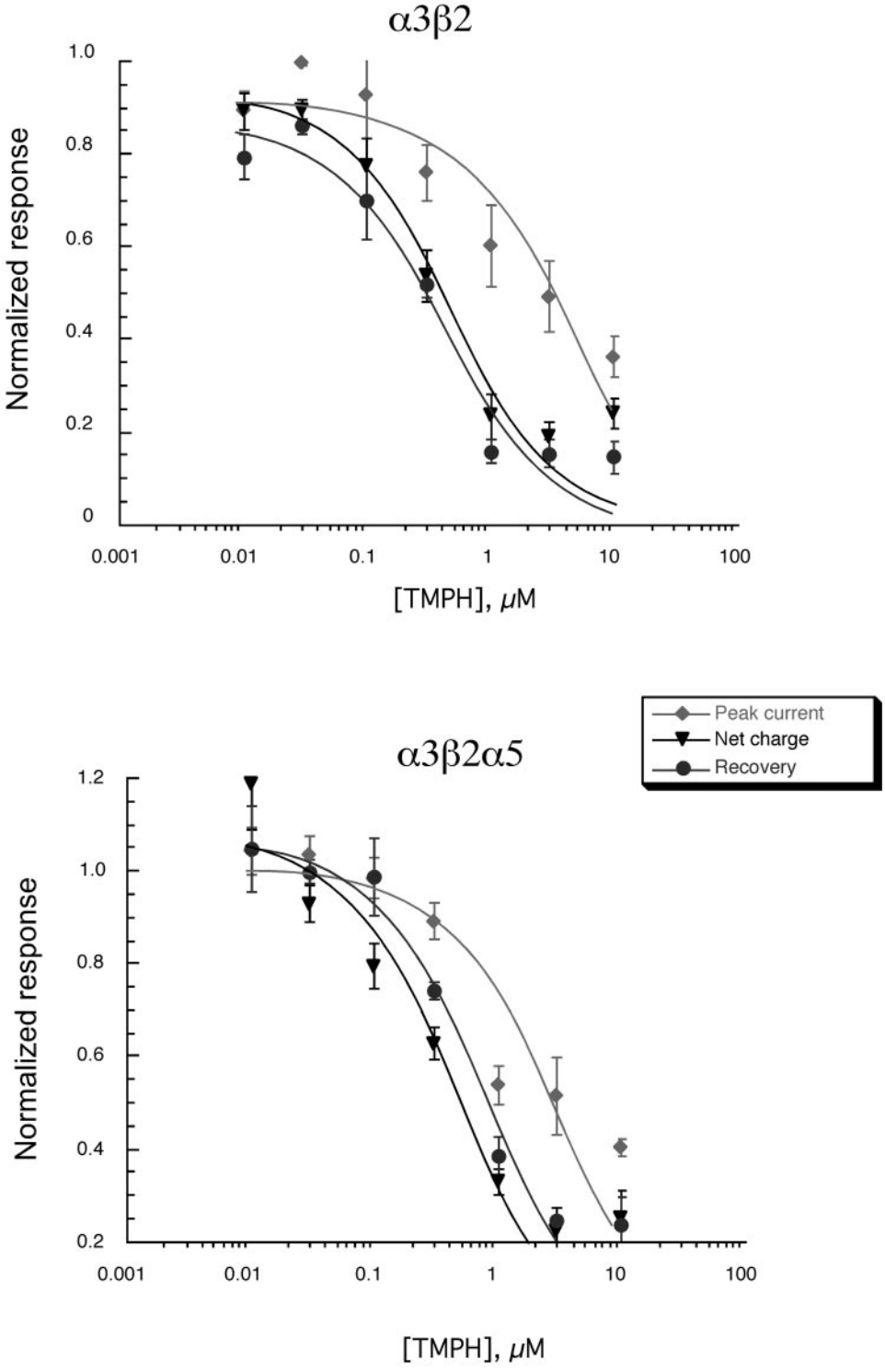

Fig. 6. TMPH inhibition of responses obtained from oocytes expressing human neuronal nAChR subunits. Shown are the averaged normalized data (±S.E.M.; $n \geq 4$) from oocytes expressing human $\alpha3\beta2$ or $\alpha3\beta2\alpha5$ subunits (top and bottom, respectively) to the coapplication ACh and a range of TMPH concentrations. Three values are plotted in each of the concentration-response curves: the peak current amplitude of the coapplication response, normalized to the peak amplitude of the previous ACh control (♦); the net charge of the coapplication response, normalized to the net charge of the previous ACh control (▼); and the peak current amplitude of the ACh control response obtained after the TMPH/ACh coapplication, normalized to the peak amplitude of the previous ACh control (●). The control ACh concentrations used were 30 and 1 μM for $\alpha3\beta2$ and $\alpha3\beta2\alpha5$ expressing oocytes, respectively.

mon ancillary subunits (α5, α6, or β3) resulted in more readily reversible inhibition. Sequence in the pore-forming second transmembrane domain (TM2) is important for regulating sensitivity to other noncompetitive inhibitors, including mecamylamine and BTMPS, which is structurally related to TMPH (Francis et al., 1998; Webster et al., 1999). As shown in Fig. 10A, one point of sequence difference that stands out between β2 and β4 compared with the other neuronal nAChR is at the 10′ position (i.e., the 10th residue within the second putative transmembrane domain; Miller, 1989). In particular, there is an alanine in β2 and β4 at this site and either a serine or threonine in subunits associated with reduced sensitivity to TMPH.

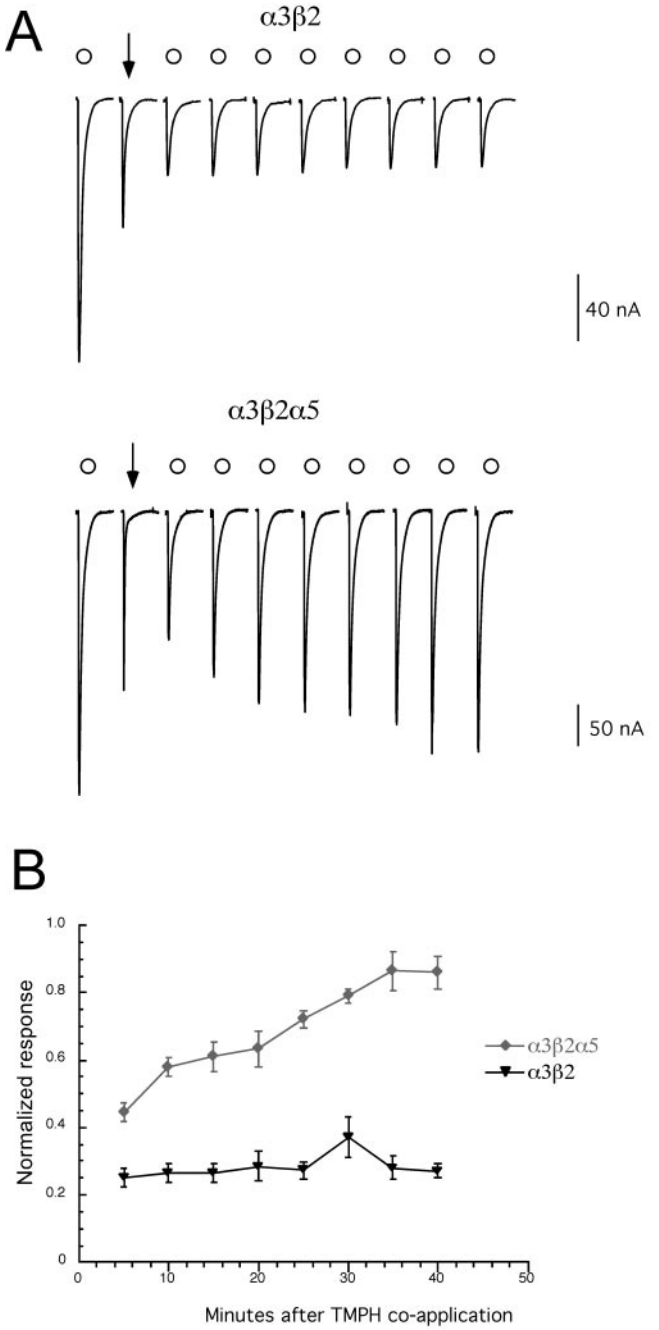

Fig. 7. Recovery of human α5-containing $\alpha3\beta2$ receptors from TMPH-produced inhibition is rapid compared with the recovery of receptors formed with $\alpha3\beta2$ subunits alone. A, representative traces obtained from oocytes expressing human $\alpha3\beta2$ or $\alpha3\beta2\alpha5$ subunits. After an initial application of ACh alone (○), a single coapplication was made of ACh and 1 μM TMPH (arrow). Recovery was evaluated by making repeated control ACh applications at 5-min intervals (open circles). B, normalized average responses of oocytes expressing $\alpha3\beta2$ or $\alpha3\beta2\alpha5$ receptors (±S.E.M.; $n \geq 4$) to repeated applications of ACh alone, after a single application of ACh plus TMPH (as in A). Peak currents are plotted, normalized to the ACh control response recorded before the ACh/TMPH coapplication. Note that the traces in A are shown on the same time scale as the x-axis in B.

We coexpressed α3 and a previously published β4 mutant (Webster et al., 1999) that contains a threonine substitution at the 10′ site. Although these receptors were strongly inhibited during a coapplication of 100 μM ACh and 30 μM TMPH, there was significant recovery after a single 5-min washout (Fig. 10B). The $\alpha3\beta4$10′T receptors recovered from TMPH inhibition with an estimated time constants of 25 ± 3 min, whereas for $\alpha3\beta4$ wild-types the estimated time constant for recovery was 450 ± 50 min (Fig. 10C, wild-type data from Fig. 3 shown for comparison).

Selective Inhibition by TMPH of Mixed Receptor Responses. Oocytes injected with a combination of α7 RNA and α3 plus β4 RNA show responses that exhibit both fast and slow components (Fig. 11A), hypothetically representing two populations of receptors. When these receptors are expressed separately, α7 receptors show only transient block by TMPH, whereas $\alpha3\beta4$ receptors show prolonged blockade. When TMPH and ACh are coapplied to an oocyte injected with all three subunits, the rapid component of the response, presumably corresponding to the α7 receptors is resistant, as can be seen after a 5-min washout. In contrast, most of the slow component of the mixed response was eliminated by the ACh/TMPH coapplication.

Note that with a simple coapplication protocol, a large transient current is evoked that we would hypothesize to be caused, at least in part, by activation of both α7 and non-α7 receptors before the use-dependent effects of TMPH. However, because α7 receptors activate on the leading edge of the solution exchange (Papke and Thinschmidt, 1998; Papke and Papke, 2002), when the TMPH concentration would still be relatively low, they would be somewhat protected from full TMPH inhibition during coapplication. Therefore, we also tested an alternative protocol which preapplied TMPH alone at 30 μM before the coapplication of 30 μM TMPH and 1 mM ACh. With this protocol (Fig. 11B), the response was very effectively inhibited during the ACh/TMPH coapplication. There was significant recovery after a 5-min washout, and the recovered response had the rapid kinetics of a pure α7 response, indicating prolonged inhibition of the $\alpha3\beta4$ receptors selectively.

Neurons in the rat septum vary in their nAChR expression in ways that are correlated to their physiological and neurotransmitter phenotypes. Septal neurons that have fast firing rates, likely to be GABAergic, often have both fast and slow components to their ACh-evoked responses, with the fast component blockable by methyllycaconitine (Thinschmidt et al., 2004; Henderson et al., 2005). Figure 11C shows the ACh-evoked response from a septal neuron recording in a fresh brain slice. The coapplication of TMPH and ACh evoked a relatively small response, suggesting that TMPH was an effective inhibitor of the neuronal nAChR in this ex vivo preparation. During the coapplication peaks were reduced to 17 ± 3% of the original average response (n = 2) and the net charge of the coapplication responses were likewise reduced to 15 ± 10%. After 3 min of washout after the TMPH appli-

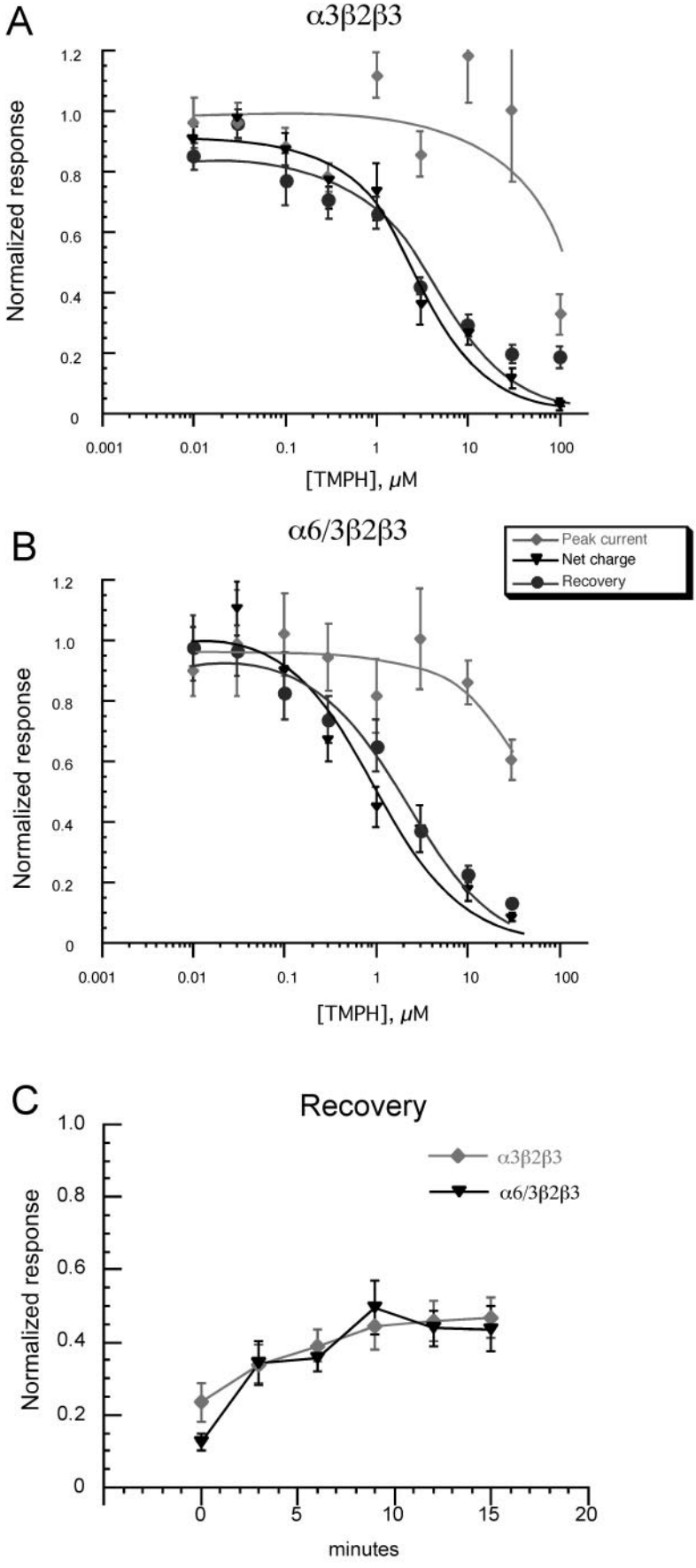

Fig. 8. TMPH inhibition of responses obtained from oocytes expressing $\beta 3$ and chimeric $\alpha 6/\alpha 3$ subunits. Shown are the averaged normalized data (±S.E.M.; $n \geq 4$) from oocytes expressing human $\alpha 3\beta 2\beta 3$ or $\alpha 6/3\beta 2\beta 3$ subunits (A and B, respectively) to the coapplication ACh and a range of TMPH concentrations. Three values are plotted in each of the concentration-response curves: the peak current amplitude of the coapplication response, normalized to the peak amplitude of the previous ACh control (♦); the net charge of the coapplication response, normalized to the net charge of the previous ACh control (▼); and the peak current amplitude of the ACh control response obtained after the TMPH/ACh coapplication, normalized to the peak amplitude of the previous ACh control (●). The control ACh concentration used was 100 μM. C, progressive recovery of oocytes expressing human $\alpha 3\beta 2\beta 3$ or $\alpha 6/3\beta 2\beta 3$ subunits. Data at $t = 0$ represents the average inhibition of peak currents during the coapplication of 100 μM ACh and 10 μM TMPH. Following points represent the responses to subsequent applications of 100 μM ACh alone at 5-min intervals. Points represent the average (±S.E.M.) of at least four oocytes, and the data were normalized to the peak responses obtained 5 min before the ACh/TMPH coapplication.

cation, there was a differential recovery of peak and net charge. Peaks amplitude had returned to 95% ± 1% of the control amplitude, whereas there was still a 43 ± 9% inhibition of the net charge. As shown in the figure inset, most of that net charge was associated with the α7-like component of the current.

Discussion

Our experiments show that TMPH is a potent noncompetitive antagonist of neuronal nAChR. Its properties are in many ways similar to its bis analog BTMPS (Papke et al., 1994), except that TMPH can produce both use-dependent and for some receptor subtypes (notably, the abundant $\alpha4\beta2$ subtype), inhibition, that does not require prior channel activation. Such use-independent inhibition, coupled with slow reversibility suggests that relatively low steady concentrations of TMPH could profoundly downregulate the function of sensitive nAChR subtypes of the brain, beyond the levels that might be achieved by activity-driven inhibition.

Although experimental agonists and antagonists are the most basic tools of pharmacology, agents with known selectivity for specific receptor subtypes are markedly better tools for understanding the molecular substrates of brain function and potential therapeutic targets. TMPH may be just such a tool for helping us understand brain nicotine receptors. However, neither BTMPS nor the prototypical ganglionic blocker mecamylamine has been tested on the same array of defined subunit combinations as were used in the current study, so

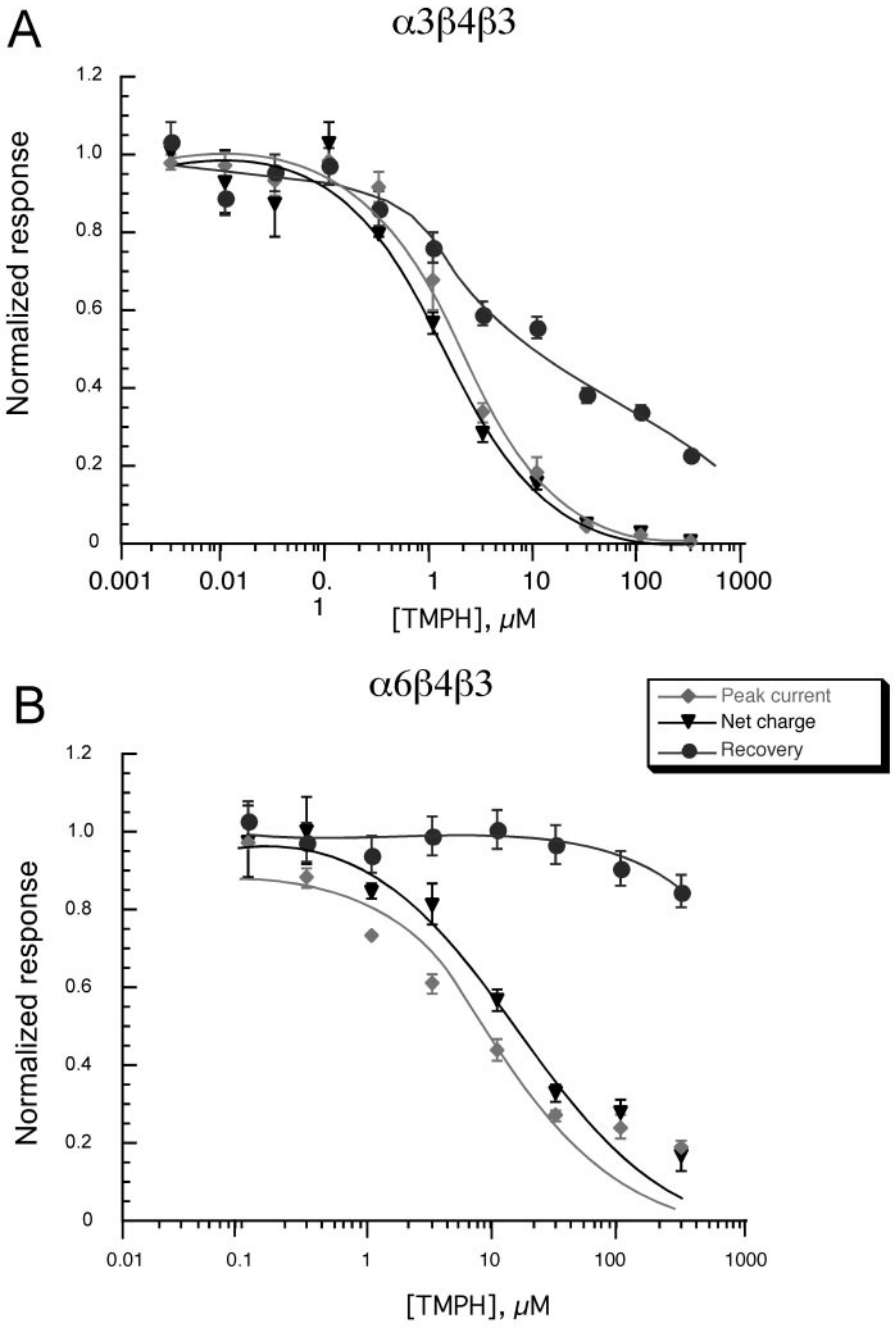

Fig. 9. TMPH inhibition of responses obtained from oocytes expressing $\beta4$, $\beta3$, and either $\alpha3$ (A) or $\alpha6$ subunits (B). Shown are the averaged normalized data (±S.E.M.; $n \geq 4$) to the coapplication 100 μM ACh and a range of TMPH concentrations. Three values are plotted in each of the concentration-response curves: the peak current amplitude of the coapplication response, normalized to the peak amplitude of the previous ACh control (♦); the net charge of the coapplication response, normalized to the net charge of the previous ACh control (▼); and the peak current amplitude of the ACh control response obtained after the TMPH/ACh coapplication, normalized to the peak amplitude of the previous ACh control (●). Note that the recovery data for oocytes expressing $\alpha3$, $\beta4$, and $\beta3$ could not be fit to a one site model. The curve fit show is for a two-site model with approximately 15% fit to an IC_{50} value of 1 μM and 85% fit to an IC_{50} value of 30 μM.

the challenge remains to better understand the activity of these inhibitors.

In recent years, the nomenclature for brain nAChR has been changing in such a way as to reflect our acknowledged uncertainty about the exact subunit composition of brain nAChR. What were previously referred to as $\alpha4\beta2$ receptors are now often $\alpha4\beta2$* or even just $\alpha4$* receptors (Tapper et al., 2004), where the asterisk indicates the uncertain presence or absence of such ancillary subunits that we show determine the reversibility of TMPH inhibition. The present studies show the potential utility of TMPH as an experimental tool that may allow us in some cases to remove the asterisk and in other cases to confirm its appropriateness.

The data obtained with the $\beta4$ 10′ mutant point to the importance of the neuronal $\beta2$ and $\beta4$ subunit TM2 sequence for defining the specificity of ganglionic blockers, and suggests at least some mechanistic similarities between TMPH inhibition and inhibition by mecamylamine (Webster et al., 1999). The apparent requirement for an alanine at that level of the pore suggests that a hydrophobic interaction may be the basis for long-lived inhibition by TMPH. Although it is a pharmacological convenience to have ganglionic blocking drugs that selectively inhibit neuronal receptors based on the β subunit sequence, presumably this crucial sequence element plays some important, albeit unknown, functional role in vivo. Moreover, just as this site makes a crucial distinction

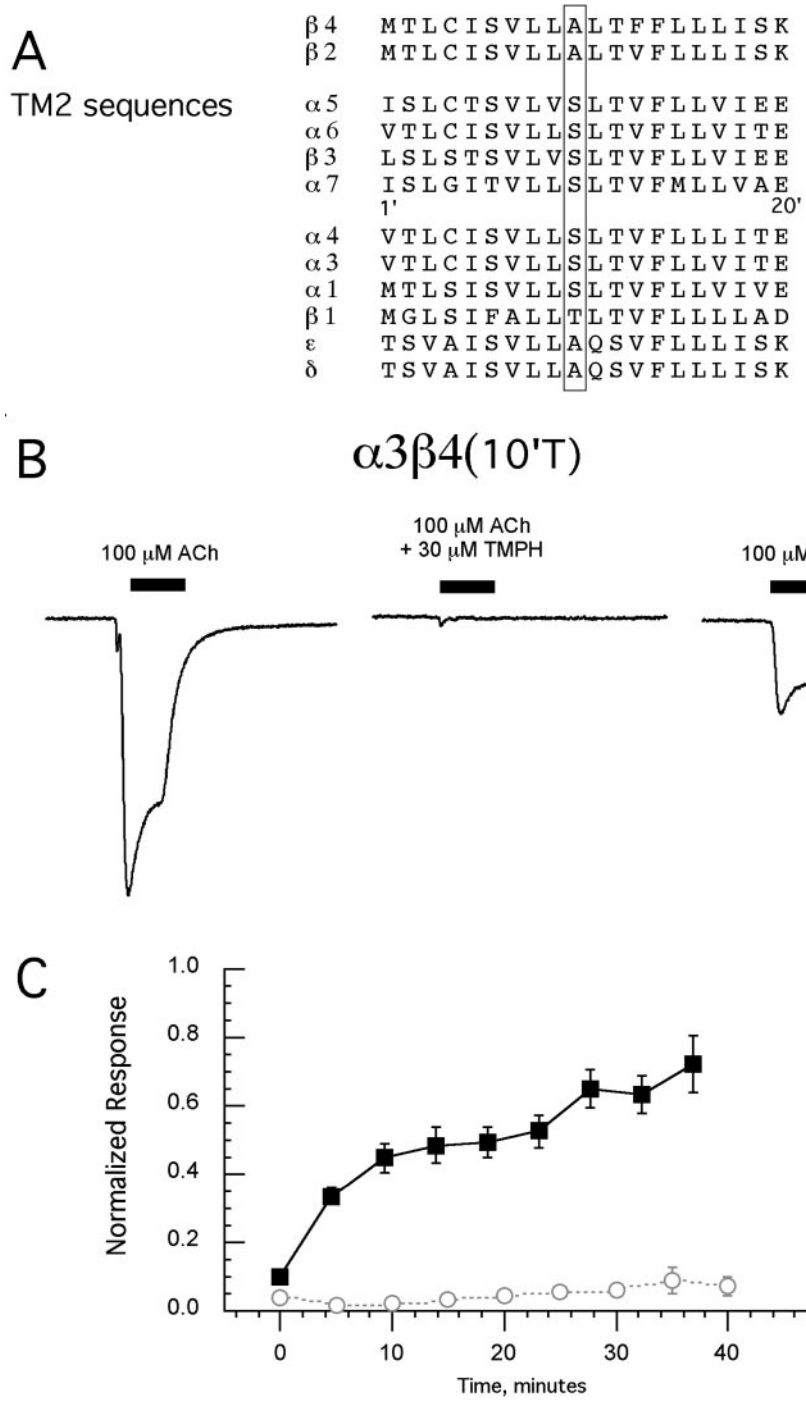

Fig. 10. Amino acid sequence in the pore-forming transmembrane domain regulates TMPH inhibition. A, sequence of TM2 domains of the nAChR subunits in this study. The sequences are aligned and numbered as proposed by Miller (1989). The 10′ site is highlighted. B, representative responses of an oocyte coexpressing $\alpha3$ and a $\beta4$ mutant in which a threonine was substituted for the alanine at the 10′ position. Shown are responses to 100 μM ACh alone, 100 μM ACh coapplied with 30 μM TMPH, and again 100 μM ACh alone. Responses were recorded from the same oocyte at 5-min intervals. During the coapplication, peak currents were reduced on average (n = 8) to 9.8 ± 1.0% of the control and the net charge during the coapplication was reduced to 7.7 ± 1.2% of the controls. C, progressive recovery of oocytes expressing $\alpha3$ and the $\beta4$ 10′T mutant. Data at t = 0 represents the average inhibition of peak currents during the coapplication of ACh and TMPH. The following points represent the responses to subsequent applications of ACh alone at 5-min intervals. Points represent the average (±S.E.M.) of at least four oocytes, and the data were normalized to the peak responses obtained 5 min before the ACh/TMPH coapplication. Data for the $\alpha3\beta4$ wild type (from Fig. 3) are provided for comparison. Time constants were estimated from exponential functions fit to the data (not shown).

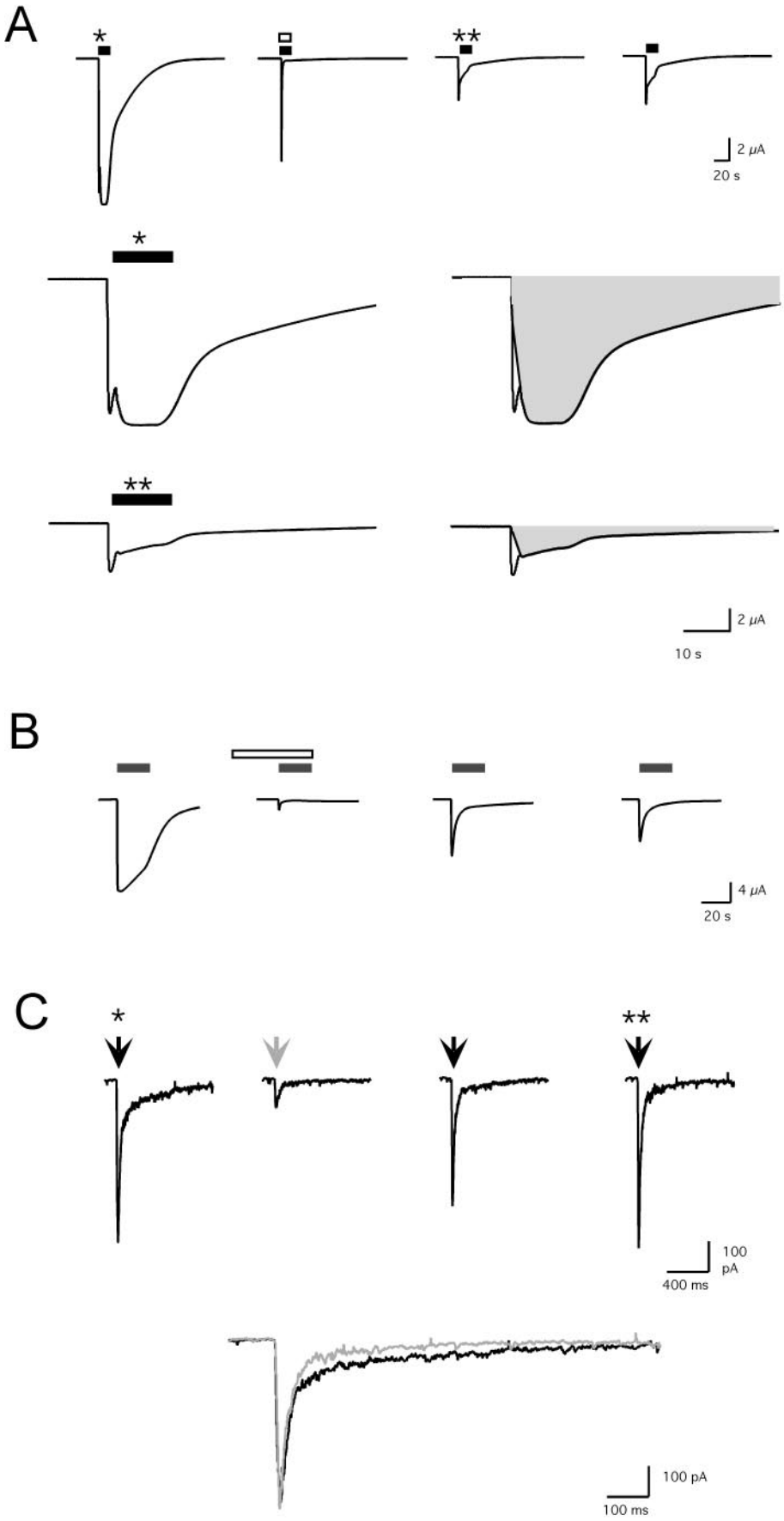

Fig. 11. Long-term inhibition of the slow components of mixed nicotinic receptor mediated responses. A, responses of an oocyte injected with RNA coding for $\alpha 7$ as well as $\alpha 3$ and $\beta 4$. The first response was evoked by the application of 1 mM ACh (closed bar). The second response was evoked by the application of 1 mM ACh plus 30 μM TMPH (open bar). The subsequent responses shown were to additional applications of 1 mM ACh alone at 5-min intervals. The expanded traces below show the two kinetic components in the ACh-evoked responses before (*) and after (**) the TMPH/ACh coapplication. In the traces on the left, an estimate of the slow component is shaded out, to illustrate the relative sparing of the fast $\alpha 7$-like component. B, responses of an oocyte expressing both $\alpha 3\beta 4$ and $\alpha 7$-type receptors. Before the coapplication-evoked response 30 μM TMPH was preapplied for 30 s to ensure that the full concentration of TMPH was present during the early $\alpha 7$-mediated phase of the mixed receptor response. Even though transient inhibition was increased with this protocol compared with the simple preapplication protocol shown in A, there was good recovery of a fast component of the mixed response after only a 5-min wash. C, responses from a patch-clamped neuron in a rat brain slice of the septum. A double-barreled picospritzer pressure application system was used with one barrel containing 1 mM ACh and the other containing 1 mM ACh and 300 μM TMPH. Three initial responses to ACh alone were obtained at 30-s intervals and the averaged response is shown (*). Two applications separated by 30 s were then made from the barrel containing both TMPH and ACh, and the average of those responses is shown. After the ACh/TMP applications, ACh alone was repeatedly applied at 30-s intervals. Shown are the averages of two traces obtained after either 60- and 90-s washout or 150- and 180-s washout (**). As shown in the overlay at the bottom, after washout the peak current amplitudes of the average response (gray) were essentially the same as the average response before the TMPH (black) application, but the late phase of the current is largely absent. Initial responses of the neuron to ACh (*) were well fit with two-exponential decay rates, with two time constants of 218 and 12 ms representing 21 and 79% of the area, respectively. After 2.5 to 3 min of recovery (**), the current decay was best fit with two time constants of 100 and 10 ms, representing 13 and 87% of the area, respectively.

between ganglionic and muscle-type receptors, it seems likely that it is of functional importance for those nAChR of the brain that incorporate the serine-containing ancillary subunits.

Based on its selectivity for long-lived inhibition of some nAChR subunit combinations and relative sparing of others, TMPH will be useful in sorting out the effects associated with complex receptor subtypes with in vitro preparations such as fresh brain slices (Fig. 11C). It may also show selectivity for blocking effects of nicotine in vivo (M. I. Damaj and R. L. Papke, manuscript submitted for publication). TMPH also may be of interest from the perspective of therapeutics because nicotinic antagonists have been proposed to be possible adjunct therapies for both Tourette's syndrome (Sanberg et al., 1998) and smoking cessation (Rose et al., 1994). The prototypical antagonist mecamylamine was used for these initial studies and the characterization of selective antagonists such as TMPH may lead the way to the development of better therapies for these, and potentially other, neuropsychiatric indications based on a more limited profile of side effects. Although the sensitivity of $\alpha 3\beta 4$ receptors to TMPH might suggest a high liability for peripheral side effects, this may not be the case because $\alpha 5$ is likely to be present in ganglionic receptors (Vernallis et al., 1993).

In conclusion, the results we report suggest that drug therapies for the inhibition of central nervous system nicotinic receptors may be developed with greater selectivity than previously appreciated. Although more selective antagonists such as methyllycaconitine are known, these generally work poorly with systemic administration. In addition to the potential therapeutic significance of TMPH, this drug may also prove to be a valuable tool to combine with selective agonists and knockout animals to further unravel the mystery of how neuronal nicotinic receptors play a role in brain function.

Acknowledgments

We thank Julia Porter Papke for technical assistance. We are very grateful to Axon Instruments Inc. for the use of an OpusXpress 6000A and pClamp9. We particularly thank Dr. Cathy Smith-Maxwell for support and help with OpusXpress.

References

Champtiaux N, Gotti C, Cordero-Erausquin M, David DJ, Przybylski C, Lena C, Clementi F, Moretti M, Rossi FM, Le Novere N, et al. (2003) Subunit composition of functional nicotinic receptors in dopaminergic neurons investigated with knockout mice. *J Neurosci* **23:**7820–7829.

Dowell C, Olivera BM, Garrett JE, Staheli ST, Watkins M, Kuryatov A, Yoshikami D, Lindstrom JM, and McIntosh JM (2003) alpha-Conotoxin PIA is selective for alpha6 subunit-containing nicotinic acetylcholine receptors. *J Neurosci* **23:**8445–8452.

Francis MM, Choi KI, Horenstein BA, and Papke RL (1998) Sensitivity to voltage-independent inhibition determined by pore-lining region of ACh receptor. *Biophys J* **74:**2306–2317.

Gerzanich V, Wang F, Kuryatov A, and Lindstrom J (1998) $\alpha 5$ Subunit alters desensitization, pharmacology, Ca^{2+} permeability and Ca^{2+} modulation of human neuronal alpha 3 nicotinic receptors. *J Pharmacol Exp Ther* **286:**311–320.

Henderson Z, Boros A, Janzso G, Westwood AJ, Monyer H, and Halasy K (2005) Somato-dendritic nicotinic receptor responses recorded in vitro from the medial septal diagonal band complex of the rodent. *J Physiol (Lond)* **562:**165–182.

Kuryatov A, Olale F, Cooper J, Choi C, and Lindstrom J (2000) Human alpha6 AChR subtypes: subunit composition, assembly and pharmacological responses. *Neuropharmacology* **39:**2570–2590.

Martin BR, Martin TJ, Fan F, and Damaj MI (1993) Central actions of nicotine antagonists. *Med Chem Res* **2:**564–577.

Miller C (1989) Genetic manipulation of ion channels: a new approach to structure and mechanism. *Neuron* **2:**1195–1205.

Papke RL, Craig AG, and Heinemann SF (1994) Inhibition of nicotinic acetylcholine receptors by bis (2,2,6,6-tetramethyl-4-piperidinyl) sebacate (Tinuvin 770), an additive to medical plastics. *J Pharmacol Exp Ther* **268:**718–726.

Papke RL and Papke JKP (2002) Comparative pharmacology of rat and human alpha7 nAChR conducted with net charge analysis. *Br J Pharmacol* **137:**49–61.

Papke RL, Sanberg PR, and Shytle RD (2001) Analysis of mecamylamine stereoisomers on human nicotinic receptor subtypes. *J Pharmacol Exp Ther* **297:**646–656.

Papke RL and Thinschmidt JS (1998) The correction of alpha7 nicotinic acetylcholine receptor concentration-response relationships in *Xenopus* oocytes. *Neurosci Lett* **256:**163–166.

Rose JE, Behm FM, Westman EC, Levin ED, Stein RM, and Ripka GV (1994) Mecamylamine combined with nicotine skin patch facilitates smoking cessation beyond nicotine patch treatment alone. *Clin Pharmacol Ther* **56:**86–99.

Sanberg PR, Shytle RD, and Silver AA (1998) Treatment of Tourette's syndrome with mecamylamine. *Lancet* **352:**705–706.

Tapper AR, McKinney SL, Nashmi R, Schwarz J, Deshpande P, Labarca C, Whiteaker P, Marks MJ, Collins AC, and Lester HA (2004) Nicotine activation of alpha4* receptors: sufficient for reward, tolerance and sensitization. *Science (Wash DC)* **306:**1029–1032.

Thinschmidt JS, King MA, Frazier CJ, Meyer EM, and Papke RL (2004) Medial septum/diagonal band cells express multiple functional nicotinic receptor subtypes that are correlated with firing frequency. *Soc Neuroscience Abstr* **30:**842.15.

Vernallis AB, Conroy WG, and Berg DK (1993) Neurons assemble acetylcholine receptors with as many as three kinds of subunits while maintaining subunit segregation among receptor subtypes. *Neuron* **10:**451–464.

Wang F, Gerzanich V, Wells GB, Anand R, Peng X, Keyser K, and Lindstrom J (1996) assembly of human neuronal nicotinic receptor $\alpha 5$ subunits with $\alpha 3$, $\beta 2$ and $\beta 4$ subunits. *J Biol Chem* **271:**17656–17665.

Webster JC, Francis MM, Porter JK, Robinson G, Stokes C, Horenstein B, and Papke RL (1999) Antagonist activities of mecamylamine and nicotine show reciprocal dependence on beta subunit sequence in the second transmembrane domain. *Br J Pharmacol* **127:**1337–1348.

Address correspondence to: Dr. Roger L. Papke, 100267 JHMHSC, 1600 SW Archer Rd., College of Medicine, University of Florida, Gainesville, FL 32610. E-mail: rlpapke@ufl.edu